

Role of Nb in 13Cr super-martensitic stainless steel

Efeito do Nb em aços inoxidáveis Super 13Cr

Xiaoping Ma

Key Laboratory for Anisotropy and Texture of Materials, North Eastern University, Shenyang, 110004, China
maxiaop@mcmaster.ca

Cheng Zhou

Key Laboratory for Anisotropy and Texture of Materials, North Eastern University, Shenyang, 110004, China
cmliu@mail.neu.edu.cn

Lijun Wang

Key Laboratory for Anisotropy and Texture of Materials, North Eastern University, Shenyang, 110004, China
lijunwang@mail.neu.edu.cn

Chunming Liu

Key Laboratory for Anisotropy and Texture of Materials, North Eastern University, Shenyang, 110004, China
373518449@qq.com

Sundaresa Subramanian

Department of Material Sci. and Engg.,
McMaster University, Hamilton, Canada L8S-4L7
subraman@mcmaster.ca

Mariana Perez de Oliveira

Companhia Brasileira de Metalurgia e Mineração (CBMM), São Paulo-SP, Brazil
mariana.perez@cbmm.com.br

Abstract

The effect of Nb microalloying on structure and physical properties of quenched and tempered 13%Cr martensitic stainless steel was investigated. Excellent strength and adequate toughness properties were obtained by 0.10 wt% Nb addition to low interstitial (N 0.01wt%, C < 0.02wt%) steel. The effect of Nb in 13%Cr steels with high N content was also studied in a commercial martensitic stainless steel sample containing higher levels of N and also alloyed with V. The microstructure, precipitate morphology and dispersion and volume fraction of reverse austenite were characterized. The strength properties obtained in the steel with 0.10%Nb are significantly higher than those of the V-containing steel. The study shows that whereas amount, size and dispersion of precipitates of microalloying elements contribute to enhanced strength, the optimum volume fraction of reverse austenite formed contributes to enhanced ductility and toughness properties. More importantly, high Nb additions to low N -13%Cr-1%Mo steel are found to improve significantly resistance against pitting corrosion significantly.

Keywords: Super martensitic stainless steel, niobium, low interstitial, nano-scale precipitate, strength properties.

Resumo

O efeito da adição de Nb, na microestrutura e nas propriedades mecânicas e de resistência à corrosão dos aços martensíticos com 13% Cr, foi investigado. Excelente resistência mecânica final e suficiente tenacidade e alongamento foram obtidos em aços contendo baixo teor de elementos intersticiais (0.01%N e C < 0.02%) e com adição de 0.10%Nb. O efeito do Nb, também, foi estudado em uma amostra industrial contendo maiores teores de N e adição de V. As propriedades mecânicas obtidas, no aço contendo 0.10% Nb, mostraram-se, significativamente, maiores que aquelas obtidas com o aço contendo V e maior teor de N. A microestrutura, morfologia e dispersão de precipitados, bem como a fração volumétrica de austenita revertida, foram, também, caracterizadas. O tamanho e a dispersão dos precipitados formados a partir dos elementos microligantes contribuem para aumentar a resistência mecânica, enquanto a formação de austenita revertida auxilia na obtenção de tenacidade e ductilidade. Quanto à resistência à corrosão por pite, o desempenho do aço 13Cr5Ni1Mo com maior teor de Nb e menor quantidade de N foi, surpreendentemente, melhor em comparação ao desempenho das demais composições estudadas.

Palavras-chave: Aço inoxidável super martensítico, nióbio, baixo intersticial, precipitados manométricos, propriedade mecânica.

1. Introduction

Martensitic stainless steels have been increasingly applied to produce oil country tubular goods (OCTG) – seamless pipes for drilling, casing and tubing – for the application in oil and gas fields with corrosive environments. They present an economical alternative against carbon steels and duplex pipes as they offer improved corrosion resistance in relation to carbon steels, being free from the use of coatings and inhibitors, and lower production costs when compared to duplex grades. Recently, a number of new weldable 13Cr martensitic grades, called “Super 13Cr”, have been developed and are also being applied to flow lines from the wellheads to the treatment stations, transporting unprocessed fluid (crude oil or gas) at high pressures and temperatures. They are based on the Fe-Cr-Ni-Mo system with 4-6% Ni, 0.5-2.5% of Mo, low C contents ($\leq 0.02\%$) and varying alloying and interstitial contents.

In stainless steels, a minimum of 12% Cr dissolved in the Fe lattice is essential to provide an adherent protective oxide layer on its surface, resulting in good corrosion resistance properties. Therefore, the precipitation of Cr rich carbides or nitrides should be avoided, as they will deplete Cr in the vicinity of the precipitates to levels below that required to form the protective oxide layer (Krauss, G.). This can be achieved by microalloying additions of Ti, Nb or V, which have higher affinity for interstitial elements than Cr, forming preferentially microalloyed carbide and carbonitrides. About 2% Mo is normally added to stainless steels to provide a good resistance to pitting corrosion. Since Cr

and Mo are ferrite stabilizing elements, in martensitic stainless steels it is necessary to make alloying additions that stabilize the austenite phase which transforms to martensite upon air cooling. Reverse austenite from tempering of martensitic stainless steel can also be formed, improving, up to certain limit, ductility and toughness (Dawood, M.).

Ni is the common alloying element used to stabilize the austenite or expand the gamma phase field. C and N are also very effective austenite stabilizers but the optimum content of these interstitial elements is determined by the specific microalloying design to achieve enhanced mechanical properties in addition to high corrosion resistance. The objective is to combine strengthening mechanisms through microalloying, while retaining ductility and toughness through an optimum fraction of reverse austenite formation in quenched and tempered martensitic stainless steel.

Figure 1A shows the phase stability diagram of Fe-13%Cr-5% Ni-0.03% C alloy, plotted using ThermoCalc Software, as a function of nitrogen content. The base chemistries of the two laboratory manufactured steels used in the present investigation are indicated on the diagram. Detailed chemical compositions are given in Table 1.

Figure 1B shows the effect of microalloying additions of M (Ti, Nb or V) on the precipitation potential and on the phase stability diagram of martensitic stainless steel. In the absence of microalloying additions, thermodynamic potential for precipitation of CrN and

Cr₂N occurs for low and high nitrogen steels. Figure 1 (B) shows the effect of microalloying additions of M (Ti, Nb or V) on the precipitation potential and on the phase stability diagram of martensitic stainless steel.

The occurrence of CrN and Cr₂N is suppressed and the precipitation of interstitial compounds of microalloying elements is promoted. The analysis of thermodynamic potential has confirmed that Nb can be used to advantage particularly in low nitrogen steels to obtain enhanced strength and toughness through control of the amount, size and dispersion of microalloyed precipitates.

The effect of high Nb (0.10wt%) additions to a low interstitial (C 0.01%, N 0.01%) to 13%Cr- 5%Ni-1%Mo base chemistry on the structure and properties of tempered supermartensitic stainless steel was investigated. The amount of reverse austenite was optimized in tempering treatments in order to achieve the required ductility and toughness in micro alloyed martensitic steels. The effects of V (0.10%) and low Nb (0.025 wt %) additions to high nitrogen (0.06 wt %) martensitic stainless steel on the structure and properties of a quenched and tempered commercial steel were also studied. Pitting corrosion studies were also carried out.

The research underscores the importance of balancing Nb additions with the level of interstitial elements (C and N) in the alloy design of 13Cr5Ni1Mo stainless steels. This will result in enhanced final strength and toughness properties with good corrosion resistance, having the best benefits from Nb microalloying.

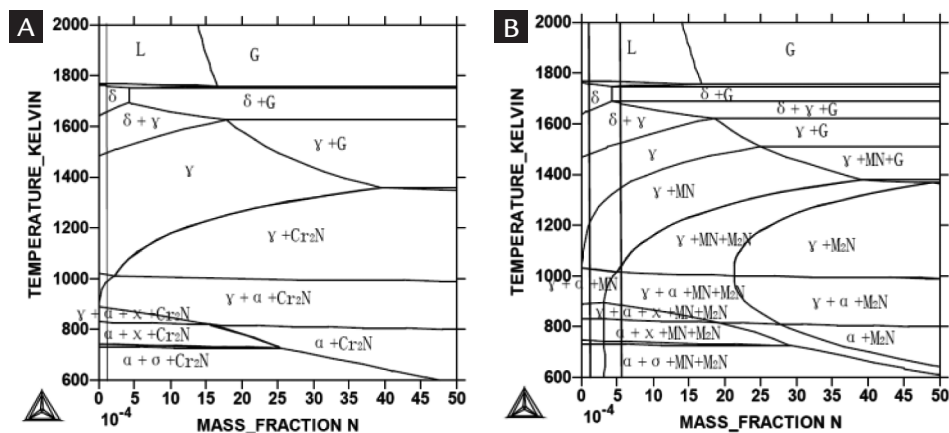


Figure 1
Phase diagram of low carbon 13Cr5Ni1Mo.
A) Fe-13.0Cr-5.0Ni-1.0Mo-N.
B) Fe-13.0Cr-5.0Ni-1.0Mo-0.03Nb-0.12V-N.

2. Materials and methods

The chemistries of two low N steels (with and without Nb) and one industrial

sample containing high N, V and Nb are summarized in Table 1. Laboratory steel

samples were made in the form of ingots, using a 100 kg vacuum induction furnace.

The ingots were hot rolled at 1200°C into plates with 12mm thickness. Normalizing was carried out at 1050°C for 0.5h, followed by tempering heat-treatment where the steels were held for 2hrs at temperatures that were varied between 550°C and 700°C. After tempering, the samples were quenched in oil.

To analyze mechanical properties, tensile and Charpy V Notch tests were performed at room temperature. The mi-

crostructure and precipitate morphology, size and dispersion were examined using conventional TEM (Philips CM12) as well as STEM, using FEI-Titan (80-300 KV). The microchemistries of the precipitates were analyzed using Energy Dispersive X-Ray Spectroscopy (EDS).

The volume fraction of the reverse austenite was measured on tempered specimens at room temperature by X-ray diffraction using Cu-K α radiation. The

evaluation of the volume fraction was determined by measuring the integrated intensities of (111) $_{\gamma}$ and (110) $_{\alpha}$ peaks of the XRD patterns, using the procedure outlined by previous researchers (LEEM, D.S.; Tanaka, M.).

The pitting corrosion resistance was evaluated electrochemically at room temperature by measuring the cyclic anodic polarization curves in distilled water with 3.5% NaCl.

Table 1
Chemistries of low and high nitrogen 13% Cr steels in wt%.

	C	Cr	Ni	Mo	N	Nb	V	Ti	Al
13Cr5Ni1Mo_0.01N	0.02	12.84	4.44	0.69	0.01	—	—	—	—
13Cr5Ni1Mo_0.01N0.10Nb	0.01	13.35	5.10	1.08	0.01	0.11	—	—	—
13 Cr5Ni1Mo_0.06N 0.025Nb0.1V	0.03	12.87	5.26	0.94	0.058	0.025	0.09	0.01	0.03

3. Results

Microstructural characterization

Microstructural and precipitate characterization of low interstitial high Nb steel

The reverse austenite volume fraction measurements for the reference steel and the one containing 0.10% Nb are shown in Table 2. It is found that reverse austenite increases with increasing tempering temperature in the two steels, reaching a peak above which it starts to decrease. Reverse austenite volume fraction peaks at different tempering temperatures for the two steel grades, being higher (650°C) for the 13Cr5Ni1Mo with 0.10% of Nb. Therefore, it appears that Nb has the ef-

fect of retarding the formation of reverse austenite, probably due to the tying up of the interstitial elements (C and N) which are austenite stabilizers.

Figure 2 refers to 0.10% Nb micro alloyed steel. Figure 2A and Figure 2B are TEM and STEM pictures which show that reverse austenite occurs on the prior austenite grain boundaries as well as within the lath structures for the sample treated at 600°C, Figure 2B illustrates in greater detail reverse austenite forming in lath

boundaries. Figure 2C shows nanoscale precipitates in the range of 10-15 nm, occurring within the lath after tempering at 700°C. Figure 2D is the precipitate of 15 nm size extracted by carbon replica and Figure 2E is the X-ray energy dispersive spectrum correspondent to the precipitate, demonstrating clearly that the precipitate is Nb rich. Similar results are obtained in samples tempered at 600°C, but the precipitates are finer, being in the size range between 5 to 10 nm.

Table 2
Volume fraction of reverse austenite in specimens tempered at different temperatures.

Tempering temperature/°C		550	575	600	625	650	700
Volume fraction of austenite/%	13Cr5Ni1Mo_0.01N	*	4.8	8.9	9.3	2.5	*
	13Cr5Ni1Mo_0.01N 0.10Nb	*	*	4.5	7.5	11.6	4.0

*X-ray diffraction pattern did not reveal the presence of reverse austenite due to very low volume fraction.

Microstructural and precipitate characterization of high nitrogen low Nb steel

The volume fraction of reverse austenite is given in Table 3 as a function of tempering temperature for the grade containing 0.06%N, 0.025%Nb and 0.10%V. The tempering temperature corresponding to the maximum volume

fraction of reverse austenite is found at 625°C. The higher amount of N – an austenitizing element, together with the lower content of Nb, appear to contribute for the peak of reverse austenite formation to be achieved earlier, at a lower

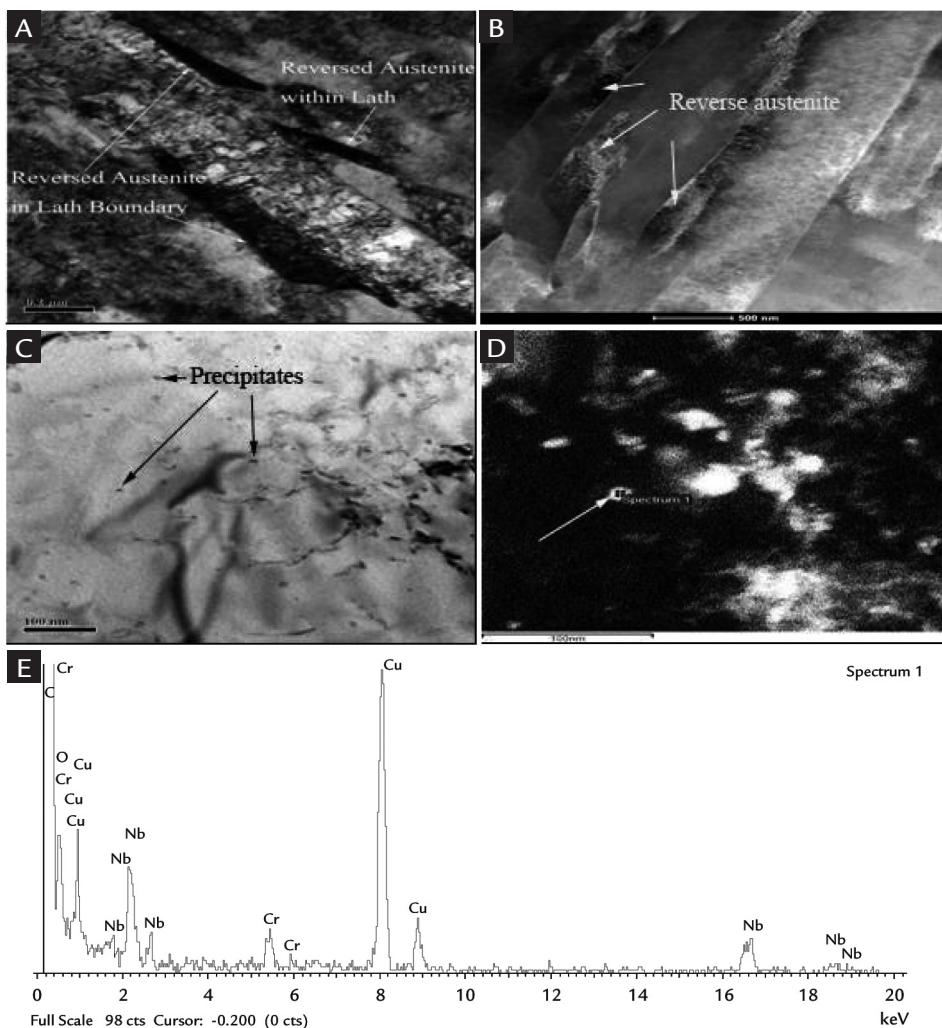
temperature than the one observed in the steel containing 0.10%Nb (650°C).

Figure 3 contains TEM images that show the occurrence of carbo-nitride precipitates in the interlath boundaries for the sample tempered at 625°C. In

Table 3
Volume fraction of reverse austenite in specimens tempered at different temperature.

Tempering temperature/°C		550	575	600	625	650	700
Volume fraction of austenite/%	13 Cr5Ni1Mo_0.06N0.025Nb0.10V	*	*	5.9	11.6	9.3	< 4.0

*X-ray diffraction pattern did not reveal the presence of reverse austenite due to very low volume fraction.



Figures 2
 A) TEM picture.
 B) STEM picture of high Nb steel tempered at 600°C, showing lath structure along with reverse austenite.
 C) TEM picture of thin foil showing precipitate morphology in 0.10% Nb steel tempered at 700°C.
 D) TEM picture of an extraction replica showing Nb rich precipitate of 15 nm size.
 E) EDS spectrum of 15nm precipitate marked in (d).

Figure 3A, the boundary carbo-nitrides are around 20 nm in diameter and 30 nm in length. In Figure 3B nanoscale precipitates of about 10 nm are observed occurring within the lath matrix. Figure 3C is the EDS spectrum from such precipitates, showing that it is rich in Cr,

Mo, V and Fe. The density and dispersion of these fine nanoscale precipitates are the effective contributors to strength. Figure 3D shows rod like and globular precipitate morphology observed on carbon extraction replica. The globular precipitates are about 10 nm size and

Figure 3E is the corresponding EDS analysis, the precipitates exhibit signals characteristic of Ti, Nb and V. Rod morphology precipitates are found to be enriched in Cr, as shown in the EDS analysis in Figure 3F.

Mechanical properties

Figure 4 shows results of the tensile and Charpy tests of the steels plotted as a function of tempering temperature. Excellent mechanical properties are obtained in 0.10%Nb and 0.01%N steel after temper-

ing at 600°C. It exhibits yield strength of 930 MPa, which is 30% higher than the control steel without Nb addition (710 MPa). Elongation is close to 20%, and toughness is about 160J. The commer-

cial sample with 0.06%N, 0.10%V and 0.025%Nb shows, at the same tempering temperature (600°C), an intermediate yield strength of 875MPa with elongation around 19% and lower toughness (140J).

Pitting corrosion properties

In Figure 5, pitting corrosion studies are presented for the three steels. It is observed that pitting corrosion resistance

of the steel containing 0.10%Nb and 0.01%N is higher than the steel used as reference (13Cr5Ni1Mo_0.01N), and

certainly superior to the steel containing 0.06%N and 0.025%Nb.

4. Discussion

Correlation of property and microstructure 13Cr5Ni1Mo_0.01N-0.10Nb

The effect of tempering temperature on microstructure and pre-

cipitation was investigated and its consequence on physical and corrosion

properties is examined to clarify the role of Nb in low interstitial (C 0.01%;

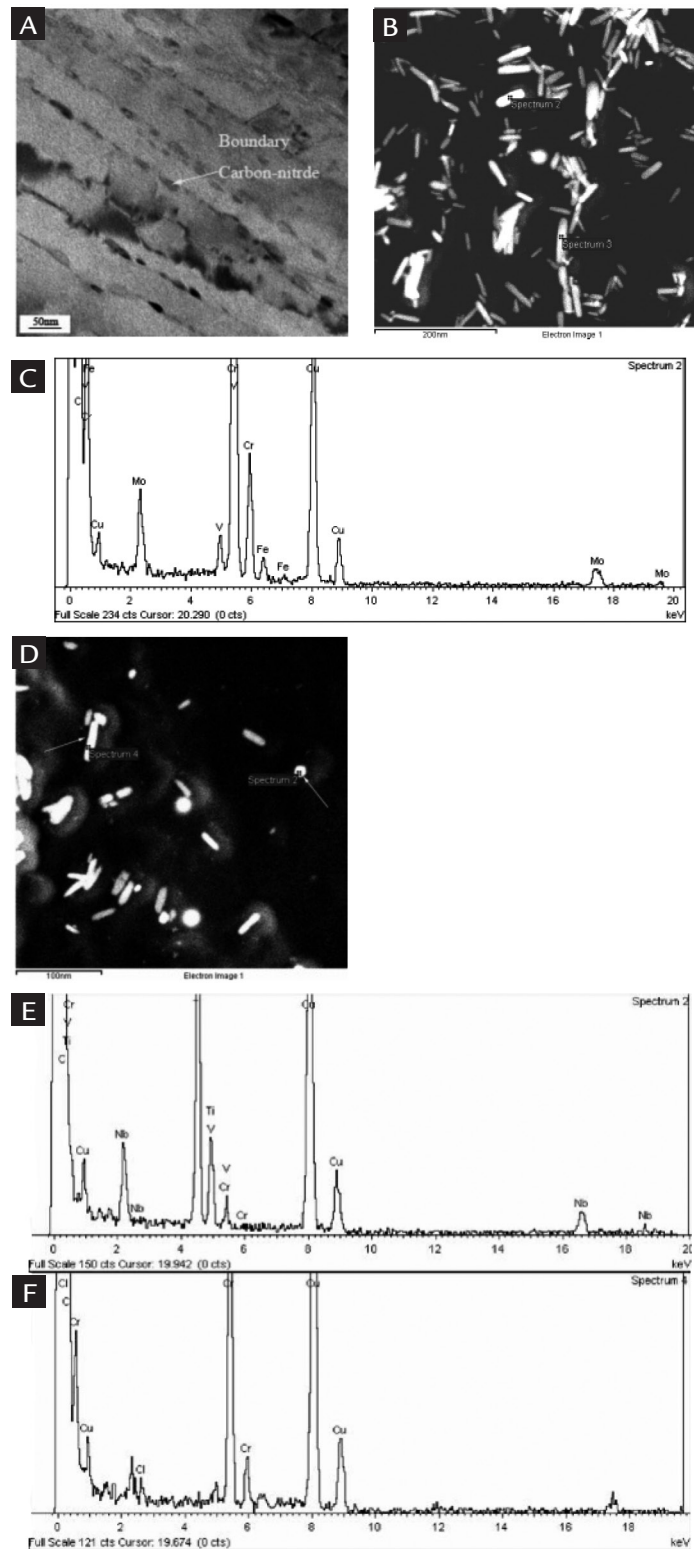


Figure 3

- A) TEM picture of thin foil showing precipitates morphologies of 13Cr5Ni1Mo-0.06N0.025Nb0.10V tempered at 625°C showing interlath precipitates.
- B) TEM picture of precipitates on carbon extraction replica showing rod morphology.
- C) EDS (Spectrum 2) of the precipitate indicated on (b).
- D) TEM picture of extraction replica.
- E) EDS spectrum of globular precipitate (Spectrum 2) in (d).
- F) EDS spectrum of rod-like precipitate indicated in (d) showing X-ray signals characteristic of Cr.

N 0.01%) base chemistry of martensitic stainless steel.

The microstructure is lath structure, characteristic of tempered martensite, exhibiting also reverse austenite. The volume fraction of reverse austenite increases with tempering temperature up to 650°C, above which the formation of secondary martensite occurs, decreasing the amount of reverse austenite.

Previous research has shown that ductility and toughness increases with

the volume fraction of reverse austenite in 13%Cr martensitic stainless steel (Bilmes, P. D et al). Thus, reverse austenite volume fraction can be used to confer ductility and Charpy toughness to the steel. This has been confirmed by the toughness measurements in Figure 4 D. The absorbed energy in the Charpy tests is higher at tempering temperatures of 650°C, for the grade with 0.10%Nb, and is close to 625°C for the other two grades tested. When this is analyzed together with measurements

of reverse austenite volume fraction from Table 2 and 3, the temperatures where the highest energy is absorbed are in agreement with the temperatures where the highest volume fraction of reverse austenite has been measured.

Regarding precipitates morphology and distribution, 13Cr5Ni1Mo_0.01N-0.10Nb tempered at 600°C exhibits a high density of nanoscale precipitates in the size range of 5-10 nm. The samples tempered at 700°C showed slightly coarser precipi-

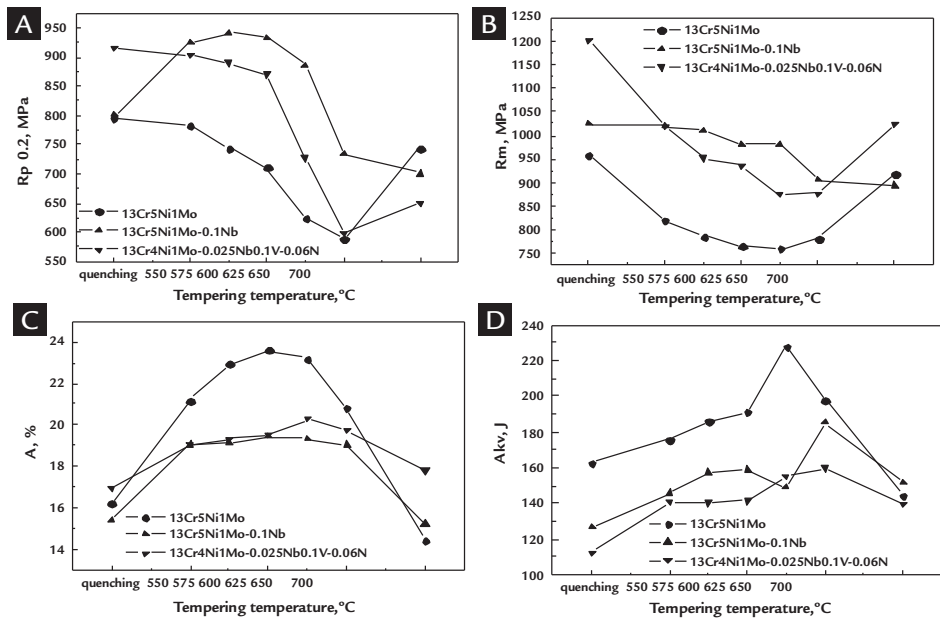


Figure 4
Mechanical properties as a function of tempering temperature of the three studied steels:
A) Yield strength (Rp0.2).
B) Ultimate tensile strength (Rm).
C) Elongation (A%).
D) Charpy tests (Akv).

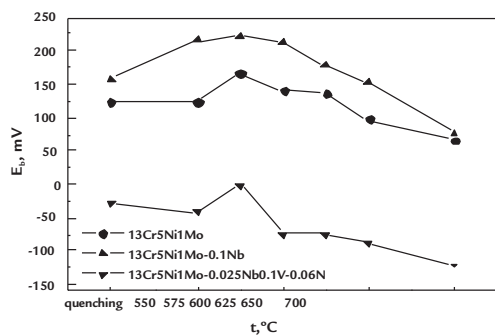


Figure 5
Pitting corrosion resistance (E_b) plotted as a function of tempering temperature. Higher E_b is indicative of higher resistance to pitting corrosion.

tate in the size range of 10-15 nm. These precipitates are confirmed to be Nb rich in Figure 2D and E.

At lower tempering temperature, the precipitates are even smaller than 5nm. These are considered to be effective in pinning the dislocations, thereby inhibiting recovery in accordance with physically based modeling of precipitate interactions with recovery (Zurob, H.S. et al). There is a significant increase in yield strength on tempering the 0.10% Nb steel at 550 and 575°C respectively, whereas there is

a significant drop in yield strength in the control steel without Nb.

This increase in yield strength upon tempering is attributed to pinning of dislocations by nanoscale precipitates of less than 5 nm, which retards the recovery of martensite. Upon tempering at 600°C, the dislocations are unpinned by coarsening of precipitates. According to Ashby-Orowan model for precipitate strengthening, strength increment in excess of 100 MPa can be obtained even at small precipitate fraction (<0.0005%) when the precipitate

size is around 5 nm (Gladman, T). Thus, the high density and good dispersion of the Nb-rich precipitates observed in the 0.10%Nb steel matrix at the tempering temperature of 600°C, can explain the significant strengthening observed in such steels when compared to the reference steel (13Cr5Ni1Mo_0.01N).

High Nb-low N steel exhibits a combination of high yield strength (930MPa), good ductility (19.4%) and good toughness (160 Joules) on tempering at 600°C.

13Cr5Ni1Mo_0.06N-0.025Nb-0.1V

The effect of microalloying additions of V (0.10%) and lower Nb (0.025%) to a 13Cr steel with higher interstitial content (N~0.06%) is to produce a large volume fraction of precipitates prior to tempering. According to thermodynamic analysis for precipitation carried out in the present work using quantitative modeling, the thermodynamic potential for precipitation of NbN

in 0.06N-0.025Nb steel starts at 1220°C, closely followed by VN at 1200°C.

TEM characterization of precipitate morphology and dispersion shows fine rod like precipitates (10 nm diameter and 30-60 nm length) occurring in prior austenite grain boundary and in interlath boundaries. Most of the precipitates are formed prior to tempering as they are seen

in all tempered specimens. The important distinction between this steel and the one with lower N and higher Nb content is in the nanoscale precipitates in the size range of 5-10 nm that are formed during tempering in the steel containing higher Nb, which, as discussed in the previous section, is very effective in imparting additional strength.

Pitting corrosion resistance

The resistance to pitting corrosion of the steel containing 0.10%Nb

and 0.01%N is far superior to those of the steel with lower Nb content

and higher N and V addition. This is also observed when pitting corro-

sion is compared to the steel used as reference, with low interstitial content

(N~0.01%) and without microalloying addition. More basic science work is

required to clarify the mechanisms involved.

5. Conclusions

- Adding high Nb (0.10%) to low interstitial (N- 0.01%) steel promotes a high density of nanoscale precipitates (5-15nm) enriched in Nb, enhancing mechanical properties in 13% Cr steel. Among the several tempering treatments, the one made at 600°C presented the best correlation between higher strength and sufficient elongation and toughness. This is attributed to a precipitation strengthening mechanism. The yield strength and ultimate tensile strength obtained by tempering the steel containing 0.10%Nb and low interstitial content at 600-625°C surpass those obtained with the steel micro alloyed with 0.10%V, 0.06%N

and 0.025%Nb.

- The effect of higher tempering temperature is to increase the volume fraction of reverse austenite, which is beneficial for promoting ductility and toughness. Addition of Nb retards the formation of the reverse austenite and enhances strength through precipitation hardening. Therefore, in order to have steel with higher strength and good toughness and elongation, an optimization between alloy design and processing parameters is essential.
- Regarding corrosion resistance, the tests performed showed that the steel containing 0.10%Nb and 0.01%N has superior pitting corrosion resistance in

relation to the other two steels studied, further studies are necessary in order to understand the mechanisms involved in this phenomenon.

- High Nb- low N design offers unique advantage to obtain an excellent combination of enhanced strength, good toughness and enhanced corrosion properties in supermartensitic stainless steel. It exhibits yield strength of 930 MPa, which is 30% higher than the steel reference (710 MPa) with no microalloying addition, with enough elongation (close to 20%) and toughness (160J).

6. Acknowledgements

We acknowledge with grateful thanks (i) funding support by CBMM, Brazil, (ii) the award of a scholarship by China Scholarship Council for the student

Xiaoping Ma to do research at McMaster University, (iii) help with steels and preparation of materials by Chinese steel companies. We wish to thank sincerely

Dr. X.Wang, Dr. Carmen Andrie and Dr. Glynis de Silveira for helping with TEM studies, and Mr. W. Gong for the assistance with XRD analysis.

7. References

- BILMES, P. D., SOLARIB, M., LLORENTE, C. L. Characteristics and effects of austenite resulting from tempering of 13Cr–NiMo martensitic steel weld metals. *Materials Characterization*, v. 46, Issue 4, p.285-296, April 2001.
- DAWOOD, M., MAHALLAWI, I. S. El, ABD, M. EL AZIM, KOUSSY, M.R. EL. Thermal aging of 16Cr – 5Ni – 1Mo stainless steel Part 2 - Mechanical property characterisation. *Materials Science and Technology*, v. 20, n. 3, p. 370-374, March 2004.
- GLADMAN, T. Physical metallurgy of microalloyed steels. *The Institute of Materials Publication*, U.K. 1997, p.273.
- KRAUSS, G. Steels-heat treatment and processing principles. *ASM publication*, 1990.
- LEEM, D.S., LEEB, Y.D., JUNC, J.H., CHOI, C. S. Amount of retained austenite at room temperature after reverse transformation of martensite to austenite in an Fe–13%Cr–7%Ni–3%Si martensitic stainless steel. *Scripta Materialia*, v. 45, Issue 7, p. 767-772, 10th October 2001.
- TANAKA, M., CHOI, C.S. *Trans. ISIJ*, n. 12, p. 16, 1972.
- ZUROB, H.S., ZHU, G., SUBRAMANIAN, S.V., PURDY, G.R., HUTCHINSON, C.R., BRECHET, Y.J.M. Analysis of the effect of mn on the recrystallization kinetics of high Nb steel: an example of physically-based alloy design. *ISIJ* 45, p.713-722, 2005.

Paper submitted to INOX 2010- 10th Brazilian Stainless Steel Conference, September 20-22, Rio de Janeiro, Brazil. Revised accepted August, 09, 2012.